NBSIR 76-1161

High Voltage Microscopy of the Reduction of Hematite to Magnetite

---

P. R. Swann and N. J. Tighe

Department of Metallurgy and Materials Science
Imperial College of Science and Technology
London, SW7 2BP, England

Inorganic Materials Division
Institute for Materials Research
National Bureau of Standards
Washington, D. C. 20234

December 1976

Interim report for Period 1971 to 1973

Prepared for
EOAR·
223/231
Marylebone Road
London, NW1
England

NBSIR 76-1161

HIGH VOLTAGE MICROSCOPY OF THE REDUCTION OF HEMATITE TO MAGNETITE

P. R. Swann and N. J. Tighe

Department of Metallurgy and Materials Science
Imperial College of Science and Technology
London, SW7 2BP, England

Inorganic Materials Division
Institute for Materials Research
National Bureau of Standards
Washington, D. C. 20234

December 1976

Interim report for period 1971 to 1973
Submitted to Metallurgical Transactions

Prepared for
EOAR
223/231
Marylebone Rd.
London, NW1
England

U.S. DEPARTMENT OF COMMERCE, Elliot L. Richardson, ***Secretary***
Edward O. Vetter, ***Under Secretary***
Dr. Betsy Ancker-Johnson, ***Assistant Secretary for Science and Technology***
NATIONAL BUREAU OF STANDARDS, Ernest Ambler, ***Acting Director***

HIGH VOLTAGE MICROSCOPY OF THE REDUCTION OF HEMATITE TO MAGNETITE

By

P. R. Swann[1] and N. J. Tighe[2]

Abstract

The microstructural changes associated with the formation of magnetite in hematite have been studied in specimens which have been partially reduced outside the microscope, thinned until electron transparent, and then examined in the normal way. Three types of structure have been observed in varying proportions which depend on the reduction temperature. At low temperatures, magnetite grows by the propagation of a cellular interface, the gas phase being transported to the cell boundary by a network of tunnels. At intermediate temperatures, magnetite plates are formed, whereas at high temperatures, both plate magnetite and blocky magnetite appear. It is proposed that the factor controlling the morphology which develops is the ratio of the cell boundary diffusivity to volume diffusivity of ferrous ions. It is noted that the decomposition morphologies of hematite and austenite have many similarities. The basic reason for this similarity is that both transformations involve substantial redistribution of elements in the solid state and the microstructures which develop are those that perform this redistribution the most efficiently at the temperatures involved.

[1] Department of Metallurgy and Materials Science, Imperial College of Science and Technology, London, SW7 2BP, England

[2] Inorganic Materials Division, National Bureau of Standards, Washington, D. C. 20234

This paper is based in part on a thesis submitted by N. J. Tighe in partial fulfillment for the degree Doctor of Philosophy at the University of London.

Introduction

The kinetics of the reduction of hematite to a porous magnetite are often discussed in terms of three rate-controlling processes, namely: (1) chemical, (2) diffusional, and (3) mixed control(1-4). Under chemical control, most of the total driving force available for the reaction is consumed by the gas-solid reaction occurring at the hematite/magnetite interface. In other words, the resistance to diffusion of the reaction gases through the porous magnetite layer to the reaction interface is negligible. If this were not the case, the reaction would proceed either under mixed control in which the chemical and diffusion steps involve approximately equal fractions of the overall driving force or under pure diffusion control in which the interfacial reaction proceeds with negligible resistance. Surprisingly, very little emphasis is given in the literature to the role of solid state diffusion processes in the hematite phase and to the nucleation event at the reaction interface. Furthermore, although the porosity of the product magnetite phase is an important feature of most theories of hematite reduction, relatively few attempts have been made to explain how this porosity develops.

In this work we have tried to gain some insight into the reduction mechanism by studying the microstructure of the unreacted hematite, the reaction interface and the magnetite product. Specimens partially reacted outside the microscope were examined after ion thinning suitable sections. Many of the electron microscope observations were correlated directly with further structures seen in the light microscope and scanning electron microscope.

Experimental Procedures

Specimens used in the reduction experiments were made from: (1) micaceous and other natural hematites, (2) pressed powder discs sintered at 1200 °C, and (3) platelets grown in a borax-flux. The micaceous hematites cleaved readily into electron transparent plates with faces parallel to the basal plane of the hexagonal hematite structure. The non-cleavable specimens were ground to form wafers 40 μm thick, ultrasonically cut into discs 3 mm in diameter and thinned for electron microscopy by ion bombardment.

A furnace was built for partially reducing bulk specimens of hematite outside the electron microscope at gas pressures up to one atmosphere. These specimens were supported in a platinum boat and could be heated in the temperature range 400 °C to 1100 °C in hydrogen atmospheres and in a wide range of CO/CO_2 mixtures. In addition, a differentially pumped environmental cell was designed and constructed in order to carry out reduction experiments in the AEI EM7 million volt microscope. The cell spans the gap between the pole piece of the objective lens and provides a 500 ml reservoir for the reducing gas around the specimen. More detailed descriptions of the cell and its performance have been given elsewhere.(5,6)

Experimental Results

Low Temperature Reduction

Single crystal plates of hematite 40 μm thick were fully reduced to magnetite at 400 °C and then prepared for electron microscope examination by ion thinning. Figure 1 shows a typical example of the microstructure

Fig. 1 Magnetite produced by reducing a single crystal of hematite in one atmosphere (101 kNm^{-2}) CO at 400°C. The electron micrograph is a cross section through the tunnel structure of several reduction colonies. The changes in orientation of the magnetite across the boundaries of the individual colonies produce the sharp changes of contrast indicated by the arrows in the micrograph.

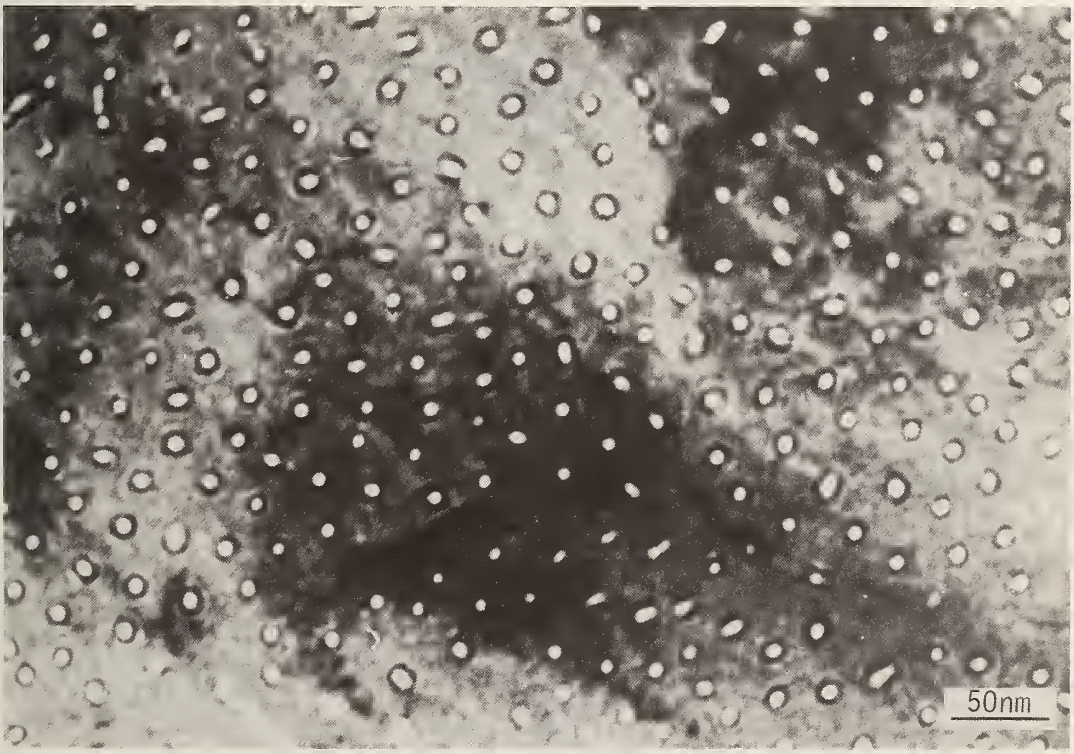

Fig. 2 High magnification view along the axes of reduction tunnels in magnetite. Note the uniformity of the tunnel spacing and diameter.

produced by this low temperature reduction. It is seen that the magnetite product is composed of cells or colonies containing a dense network of tunnels with an average spacing of about 27 nm and a mean diameter of about 8 nm. The tunnel or sponge-like structure is extremely fragile and colonies often fracture under the stresses generated by the reduction reaction. Figure 2 is a higher magnification view of the porous magnetite normal to the axes of the reduction tunnels and clearly shows the uniformity of the tunnel spacing and diameter. A light micrograph of a hematite specimen partially reduced at 400 °C is shown in Fig. 3a. Two impinging cells of magnetite have grown from the left of the field of view and the magnetite/hematite interface is roughly perpendicular to the plane of the micrograph. The specimen has been thinned until electron transparent so that the structure of the interface could be examined in the high voltage microscope. Figure 3b shows such a view and it can be seen that the tunnels extend right up to the reaction interface and are roughly perpendicular to it. The diameter and spacing of the tunnels was found to vary from one specimen to another and are thought to depend on the reducing power of the gas and the reaction temperature. At present, no consistent trends have been established and further experiments are planned to determine the exact relationship.

High Temperature Reduction

A typical electron micrograph of a hematite specimen partially reduced to magnetite at 1000 °C is shown in Fig. 4. The magnetite is present in the form of single crystal plates with habits approximately parallel to the (0001) planes. The orientation relationship is $(0001)||(111)$

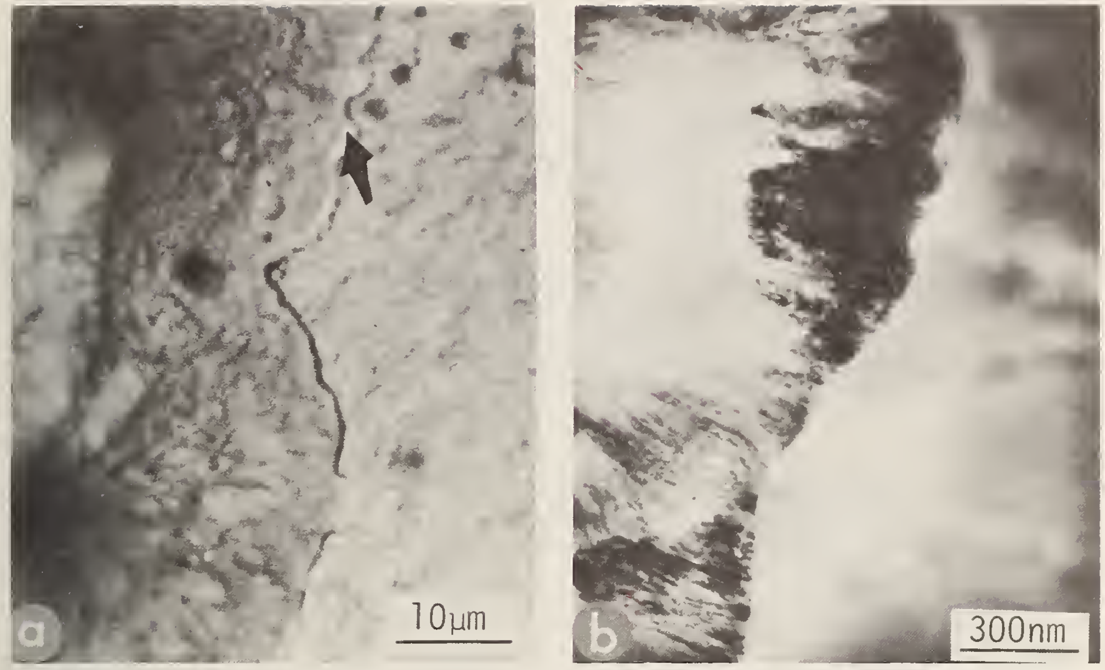

Fig. 3 (a) A light micrograph of two adjoining reduction colonies of magnetite in a partially reduced single crystal specimen of hematite. The reduction was carried out in CO at atmospheric pressure for 15 minutes at 400°C. (b) Transmission electron micrograph of region near the arrow in figure 3a showing that the fibrous tunnel structure extends right up to the reaction interface at the boundaries of the colonies.

Fig. 4 A typical electron micrograph of the "high" temperature reduction morphology in a hematite crystal partially reduced to magnetite in $CO/CO_2 = 0.125$ for one minute at 1000°C. The magnetite crystals are in the form of lenticular plates and do not contain the tunnel structure observed at lower temperatures.

and $[10\bar{1}0]||[0\bar{1}1]$. The hematite matrix shows evidence of elastic distortion around the magnetite plates and contains a recovered dislocation substructure which was not present before the reduction. Dislocations are also present at the hematite/magnetite interface. The magnetite plates do not contain the tunnel structure observed at the lower reduction temperature and must have formed, therefore, by a different mechanism.

The dislocation density of the magnetite plates depends on their rate of growth. Crystals growing rapidly under highly reducing conditions at 1000 °C usually contain a high density of dislocations as can be seen from the example in Fig. 5. It appears that accommodation stresses are significantly relaxed by diffusion and dislocation climb at the lower reaction rates used to produce the low dislocation density magnetite shown in Fig. 4.

The inset low magnification light micrograph in Fig. 5 includes the area of the adjacent electron micrograph and shows the blocky grains of magnetite which form in addition to the plates. Some of the blocky magnetite grains can be seen in the electron micrograph, but a clear example revealing their internal structure is shown in Fig. 6. It is seen that they are polycrystalline; and, from diffraction analysis, it was found that many of the individual grains are twin related.

It is interesting to note that the thickening of magnetite plates occurs predominantly by the sidewise growth of only one of the magnetite/hematite interfaces. This can be seen in Fig. 7, which is a light micrograph of the top and bottom surfaces of a fractured, partially

Fig. 5 A transmission electron micrograph of magnetite plates and nodules formed at the surface of a hematite crystal reduced in $CO/CO_2 = 0.06$ at 986°C for one minute. The magnetite plates contain a high density of dislocations which anneal out rapidly during growth. The outlined area in the inset light micrograph corresponds to the area of the electron micrograph.

Fig. 6 A high magnification view of a single magnetite nodule showing its twinned internal substructure.

reacted, 30 μm thick single crystal slab of hematite. In this figure, the hematite/magnetite interface contrast of one side of the magnetite plates is much darker than the other, e.g., at X. The reason for this difference in contrast can be understood from the scanning electron micrograph in Fig. 8 which shows that one of the magnetite plate interfaces contains rows of micropits which although not resolved in the light microscope would scatter light more strongly and appear in dark contrast. The opposite interface of the plates are free from pits and they appear in weak contrast even in the scanning image. The fissures and pits associated with the dark interface indicate that it is sessile and, thus, magnetite growth is accomplished by migration of the opposite interface. It is interesting to note from a comparison of the micrographs of the top and bottom surfaces of the broken single crystal slab in Fig. 7 that the mobile interface on one surface corresponds to the sessile on the other surface and vice versa. In other words, it appears that the mobility of a magnetite interface is different when it intersects (hkil) and $(\bar{h}\bar{k}\bar{i}\bar{l})$ hematite surfaces.

Figures 5 through 8 all show examples of magnetite plates and blocky grains, which have nucleated at the hematite surface. However, subsurface nucleation and growth also occur during high temperature reduction and an example is shown in Fig. 9. This is a light micrograph of a section through a sintered disc of hematite powder partially reduced at 1020 °C in a CO/CO_2 mixture at one atmosphere. The dark network of lines on the micrograph are the interfaces between sintered grains which have fractured during the reduction process and the grey areas are

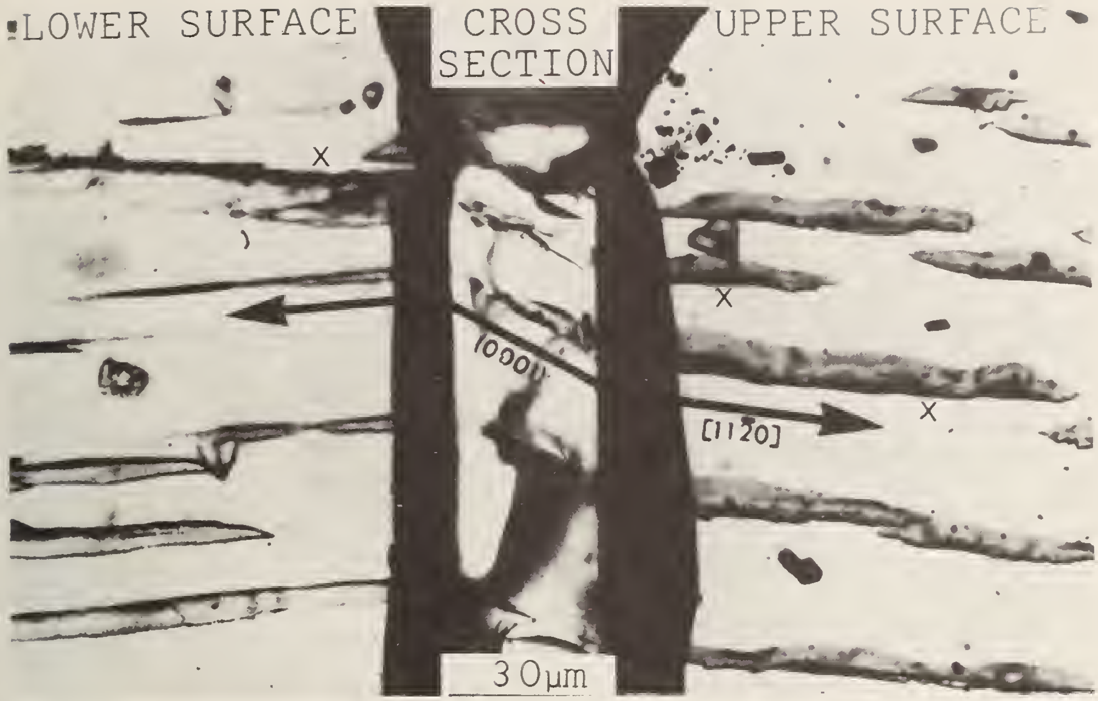

Fig. 7 A broken 30 micron thick rhombohedral-faced crystal of partially reduced hematite showing magnetite plates in cross section (i.e., in the fracture face) and matching views on opposite surfaces of the slice. The micrograph shows that the plates have an (0001) habit. Specimen reduced in $CO/CO_2 = 0.03$ for one minute at 1000°C.

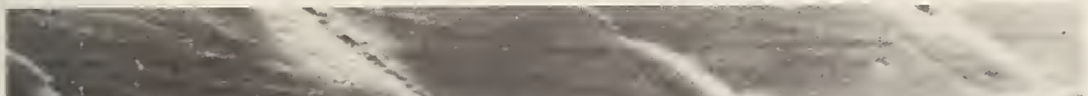

Fig. 8 A scanning electron micrograph showing the surface morphology associated with the magnetite plates seen by light microscopy in fig. 7. A surface groove or porous fracture is present where one face of the magnetite plate intersects the surface of the crystal. This morphology is responsible for the dark contrast along one edge of the plates in figure 7.

sections through magnetite plates. Most of the magnetite plates extend to the boundaries of the individual grains and plates lying totally within the grains are presumed to intersect the boundary at some point outside the plane of the section. However, in addition to the plates there are several small particles of magnetite, e.g., at X which appear to have nucleated totally within the grains. These particles could only have formed as a result of matrix diffusion through the hematite.

The above description of the high temperature reaction product is based on preliminary observations and is certainly a simplification of the actual microstructure. In reality, the structure is constantly changing during the reaction and freshly formed magnetite in the reaction zone has a different microstructure from the magnetite formed at the beginning of the reaction. For example, after some time at the reaction temperature, dislocations in the magnetite plates relax their long range stress fields by rearranging to form networks, as shown in Fig. 10. In many cases, the elastic stresses generated during reduction can lead to fracture of the magnetite before other elastic recovery processes occur. In addition, the magnetite can also recrystallize.

Similar changes also occur during aging of the low temperature reaction product. However, in this case the high surface energy associated with the tunnel structure can cause an additional discontinuous sintering reaction to take place which has a pronounced effect on the interconnectivity of pores and the pore size. It is clear that the pore size measured at the end of a complete reduction to magnetite is not a true reflection of the pore size existing at the reaction interface.

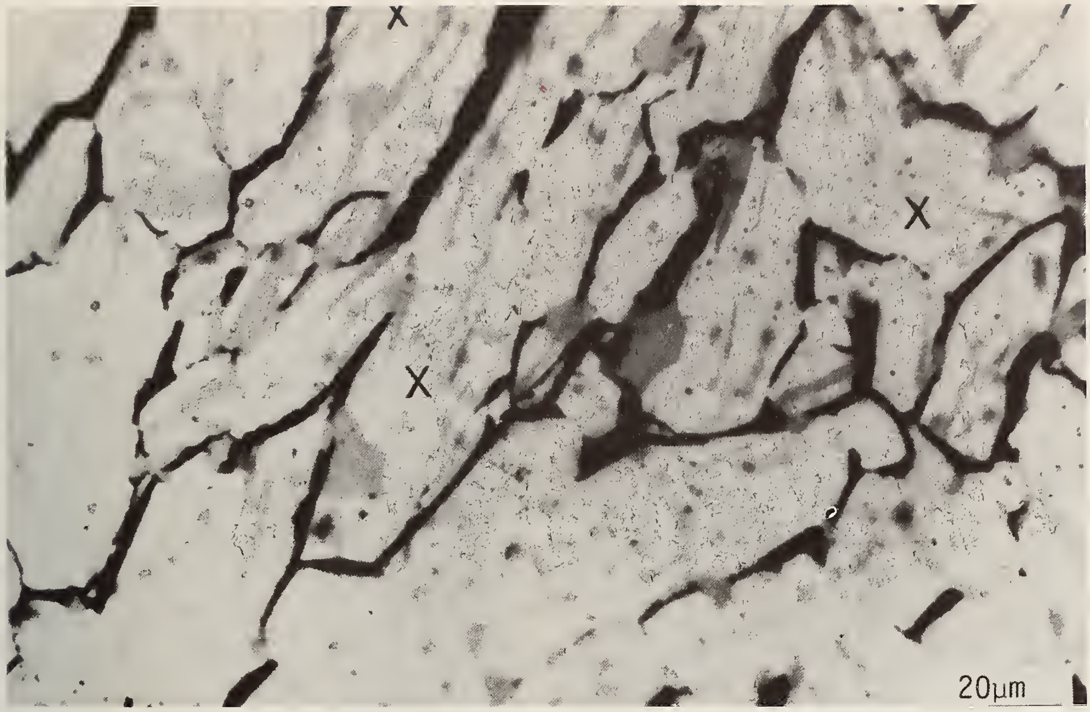

Fig. 9 A light micrograph of an area near the surface of a hematite polycrystal partially reduced to magnetite in $CO/CO_2 = 0.03$ for 10 minutes at 1020°C. Fractures are seen along the hematite grain boundaries and many magnetite plates extend from the boundaries into these grains. The micrograph shows many examples of subsurface nucleated magnetite precipitates, e.g., at X.

Fig. 10 Network of dislocations within a specimen fully reduced to magnetite at 1000°C. These networks form by a recovery process at temperatures after the reduction has occurred.

Reduction at Intermediate Temperatures

At intermediate temperatures (600-800 °C), magnetite can form by both plate and cellular growth. The light micrograph in Fig. 11a is a typical example and shows plate nuclei at X and roughly hemispherical cells possessing the tunnel structure at Y. The magnetite plates also appear to act as nuclei for the cellular structure; two examples are indicated by arrows in Fig. 11a. It is interesting to note that initially the cellular structure grows preferentially from only one side of the magnetite plates in any one grain.

Figure 11b is an electron micrograph of the plate-nucleated cellular structure in the same specimen used to obtain Fig. 11a. The original traces of the magnetite plate nuclei can be recognized by the long cracks running diagonally across the micrograph. These cracks or grooves are responsible for the lines of dark contrast seen in plates viewed in the light microscope. There is also a second system of shorter, light contrast lines steeply inclined to the main grooves. These lines appear to be enlarged tunnels in the magnetite.

Discussion

The electron microscope observations have revealed that the reduction of hematite to magnetite can occur by at least two different mechanisms, one of which predominates at temperatures below about 650 °C and the other at temperatures above 800 °C. In the temperature range 650 °C to 800 °C, both mechanisms operate in varying proportions. The experimental observations also indicate that solid state diffusional processes play a much wider role in the reduction mechanism than has been realized in

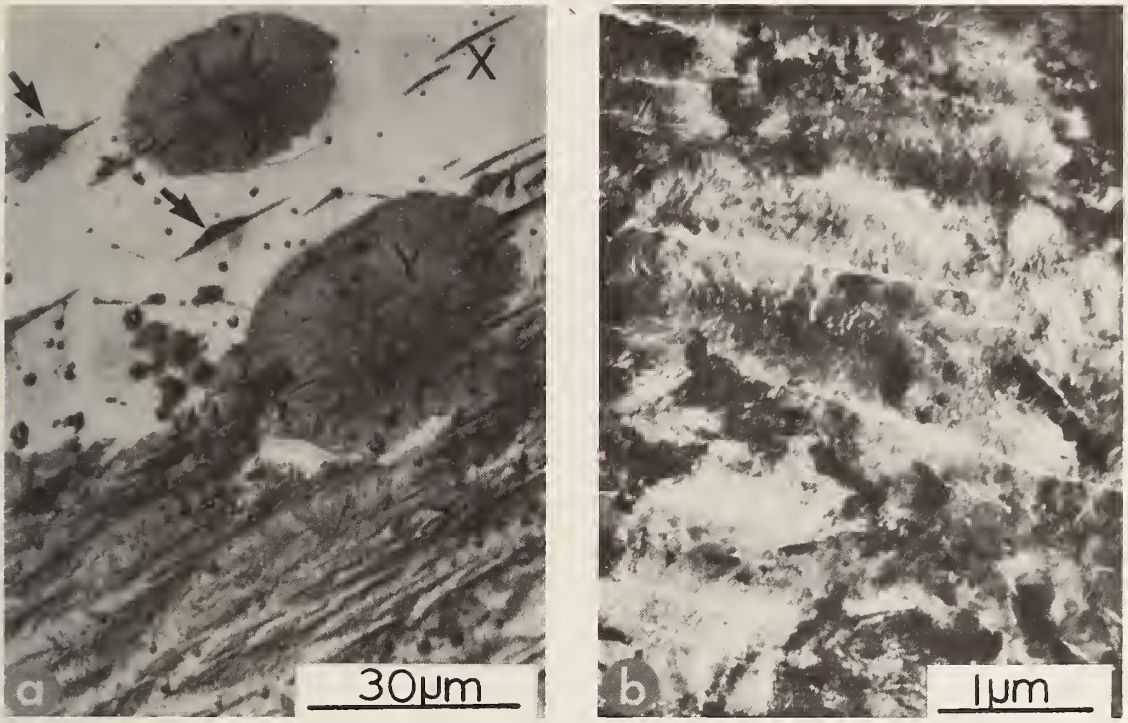

Fig. 11 (a) A light micrograph showing the typical reduction morphology of specimens partially transformed at "intermediate" temperatures. Note that the specimen contains both magnetite plates (at x) and reduction tunnel colonies (at y). The magnetite plates appear to nucleate the tunnel reaction; e.g., at points indicated by arrows. (b) A transmission electron micrograph of a colony such as y showing the central systems of fractures associated with the plate nucleus.

earlier publications. Furthermore, the microstructural changes which occur bear many similarities to well-known solid state transformations in alloys as will be discussed below.

Reduction at Low Temperatures

(a) Reduction Morphology

The most striking feature of the low temperature (400 °C-650 °C) reduction reaction is the formation of magnetite colonies having a highly branched tunnel structure extending like an arterial system from the reaction interface through the magnetite to the original hematite surface. This morphology, which is drawn schematically in Fig. 12, bears a marked similarity to that developed during the cellular decomposition of a supersaturated solid solution; e.g., the pearlite reaction in steels. In such discontinuous reactions, the incoherent boundary forming the reaction interface plays a key role by providing a rapid diffusion path for partitioning the alloy components between the two phases (7). In view of the microstructural similarity, it is possible that a similar transport mechanism may also operate during the low temperature reduction of hematite. In this case, the two components,

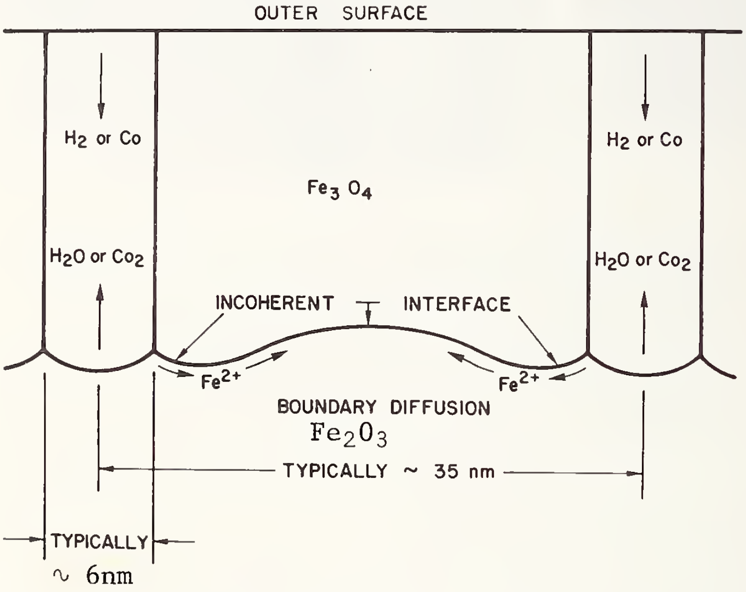

Fig. 12 Schematic diagram illustrating the mechanism of tunnel formation during the initial reduction of hematite.

iron and oxygen, must be partitioned between the magnetite phase and the gas phase according to the reaction,

$$6\ Fe_2^{3+} O_3^{2-} \rightarrow 4\ Fe_2^{3+} Fe^{2+} O_4^{2-} + O_2$$

However, in contrast to the purely solid state discontinuous reactions, the reaction interface (as shown in Fig. 1) is only partially composed of incoherent boundary, the rest being the free surface between the hematite and the gas phase. Nevertheless, this mixed interface is ideally suited for the rapid transport of the constituents involved, since the oxygen diffusion distance in the solid state can be negligible and excess ferrous ions, produced when oxygen enters the gas phase, can diffuse rapidly over the surface at the bases of the tunnels and along the hematite/magnetite boundary to their correct sites in the growing magnetite lattice.

The scale of the tunnel structure will depend on the way in which the overall energy available for reduction is distributed. Clearly, the smaller the tunnel spacing, the shorter will be the diffusion distance between tunnels, but the greater will be the energy consumed in creating the tunnel surfaces. Furthermore, as pointed out by Cahn (8), the magnitude of the interfacial mobility will exert a profound influence on the tunnel spacing by controlling the amount of boundary diffusion required to drive the interface forward. The scale of the tunnel structure is also expected to depend on temperature. With increasing temperature, the diffusion of ferrous ions into the matrix will become more important than their transport along the boundary. Thus, more of the free energy available is consumed in driving the interface forward and less remains for the creation of new tunnel surface. The tunnel spacing should, therefore, increase with rising reduction temperature.

(b) The Spacing to Diameter Ratio of the Reduction Tunnels

A primitive unit cell of the reaction product is defined in figure 13 and has edge dimensions at the reaction interface of d (i.e., the tunnel spacing) and a reduction tunnel diameter of 2r. The reduction tunnels are distributed in a hexagonal closest-packed array normal to the reaction interface (see Fig. 2) and, thus, the area of a primitive unit cell at this interface is $d^2 \cos 30°$. Since this area is intersected by just one tunnel, the tunnel density is $(d^2 \cos 30°)^{-1}$. In unit thickness of Fe_2O_3, the number of iron ions per unit cell of the reaction interface is $Nd^2 \cos 30°$, where N is the number of iron ions per unit volume of hematite. The number of oxygen ions in this initial volume before reaction is $1.50\ Nd^2 \cos 30°$ and, thus, the number which must be removed to achieve the composition Fe_3O_4 is $(1.50-1.33)\ Nd^2 \cos 30° = 0.147\ Nd^2$.

It was proposed above that a reduction tunnel is formed by the removal of oxygen into the reducing environment at its base and that the excess ferrous ion concentration so created diffuses away from the tunnel base and parallel to the reaction interface to form the surrounding magnetite. In the simplest case, it can be assumed that the cell boundary diffusivity of ferrous ions is so rapid that the flux of oxygen ions into the volume which forms the reduction tunnels is negligible. Consequently, all the oxygen ions which are removed to accomplish the change in composition from Fe_2O_3 to Fe_3O_4 are those in the tunnel volume, i.e., $1.5\ N\pi r^2$. In this case

$$0.147\ Nd^2 = 1.5\ N\pi r^2$$

giving

$$\frac{d}{r} = 5.66 \ .$$

If there is a flux of oxygen ions into the reduction tunnel volume from the matrix, the ratio d/r will be correspondingly larger than that given above. Taking x as the fraction of all oxygen ions removed during the reaction that originates from the matrix surrounding the tunnels, then the spacing to radius ratio of the tunnels becomes

$$\left(\frac{d}{r}\right)_x = 5.66 \ (1-x)^{-1/2} \ .$$

Measurements taken from micrographs such as that in Fig. 2 show that $d \simeq 27$ nm and $r \simeq 4$ nm giving $d/r = 6.75$ and $x = 0.30$. This crude calculation, which ignores the movement of any vacancies generated during the reduction reaction, indicates that about 30% of the oxygen removed originates from the matrix between the reduction tunnels.

(c) Volume Change During Low Temperature Reduction

The number of iron ions in the reacted layer is unaltered by the reaction and since the volumes of magnetite and hematite per atom of iron are almost equal, any expansion resulting from the reduction must be accounted for almost entirely by the volume of the tunnels and fissures created by fracture of the fragile reaction product. Any sintering of the reaction product during and after the reaction would tend to reduce the magnitude of the expansion. The contribution to the volume increase from the formation of tunnels will now be calculated with reference to

Fig. 13. The diffusion of iron from the tunnel region during reduction causes the original hematite layer to increase in thickness from 1 to 1 + y. If all the expansion occurs parallel to the direction of motion of the reaction front, then the primitive unit cell dimensions, d, at the reaction interface are unchanged and the volume change is simply 100y%. The value of y can be obtained by equating the volume of a tunnel, πr^2, to the volume of the extra surface layer created by the reaction $yd^2\cos 30° = \pi r^2$ and using the value for d/r given above. If the flux of oxygen into the tunnel from the matrix is negligible, i.e., x = 0, the volume increase is a maximum of 12.5%. However, if x is not negligible, the volume increase is less than 12.5% and is given by 100(1-x)/(8+x)%. For the particular example shown in figure 2 in which x was found to be 0.3, the volume increase would be 8.4%. This agrees well with magnitude of volume changes recently measured by Bradshaw and Matyas (9), who obtained values ranging from 8.6-11.7% at 600 °C and 6.1 to 7.0% at 700 °C. These values are all substantially less than 12.5%, indicating that the flux of oxygen into the reduction tunnel region from the surrounding matrix is not negligible, and also that significant amounts of sintering of the tunnels may occur during the reduction process.

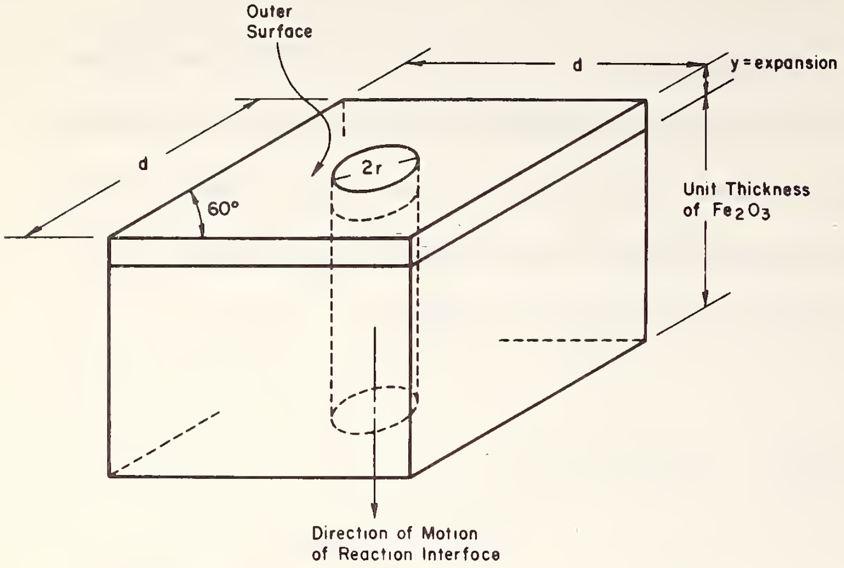

Fig. 13 Schematic diagram of a 'unit cell' of a magnetite colony formed at low reduction temperature. The reduction tunnel has a radius (r) and intertunnel distance (d).

(d) The Low Temperature Reaction Rate

The driving force for the boundary migration of a porous magnetite colony is related to the deviation from stoichiometry maintained at the hematite/gas interface at the bases of the reduction tunnels. If this does not change during the course of the reaction (e.g., gaseous diffusion along the tunnels is not rate controlling), then the driving force and, hence, the velocity of the interface would be constant. In this case, many factors at the reaction interface can control the growth rate, e.g., the rate of diffusion of ferrous ions along the magnetite/hematite interface, the rate of removal of oxygen ions from the base of the tunnels, the intrinsic mobility of the magnetite-hematite interface, boundary drag due to interaction of the interface with foreign ions. However, whichever of these factors is rate controlling, the overall reaction rate, R, would be expected to obey some form of the Johnson-Mehl(10) equation which takes impingement of neighboring colonies into account; e.g.,

$$R = 1\text{-}\exp(-kIG^3t^n)$$

where I is the nucleation rate of the magnetite colonies, G is their interface growth rate, n is the time exponent which takes on a range of values according to the conditions given by Cahn(11) in his treatment of grain boundary nucleated eutectoid reactions.

Reduction at High Temperatures

The magnetite produced at reduction temperatures above 800 °C is predominantly in the form of lenticular plates or blocky grains. The morphologies bear many similarities to the Widmanstatten plates and chunky ferrite allotriomorphs found in steels. The development of the plate morphology is indicative of growth controlled by long range diffusion. The small radius of curvature at the tip of a growing plate produces steeper concentration gradients of the diffusing species there and leads to a higher diffusion flux of ferrous and oxygen ions to and from the tip This would account for the enhanced tip velocity necessary to maintain the plate morphology during continued lengthwise growth. The sidewise growth rate of the plates appears to be controlled more by the anisotropy of interface mobility than by diffusion. The microscopic observations revealed a strong tendency for plates to lie parallel to the basal plane of the hematite and it was noted that the interface on one side of a growing plate was more mobile than that on the other side. The tendency for a groove to form where the less mobile interface intersected the hematite surface suggests that boundary diffusion plays a role in the transport of ions to and from the surface. However, it is evident from Fig. 7, which shows copious amounts of sub-surface magnetite nucleation, that the growth of plates does not depend on this type boundary diffusion.

The formation of blocky grains results from the cooperative nucleation of several grains of internally twinned magnetite. In these clusters of grains, the (0001)||(111) orientation relationship is not observed and the special low mobility-basal plane interface associated with plate growth cannot develop. As a consequence, the growth proceeds at similar rates in all directions.

Reduction at Intermediate Temperatures

At temperatures in the range 650 °C to 800 °C, cellular and plate growth occur simultaneously. The microscopic observations revealed that, in general, the magnetite nucleates in the form of plates, but subsequent growth occurs by the cellular mechanism. This results in the formation of plate-like colonies containing a dense tunnel structure radiating from the mid rib of the plate nucleus. The transition from cellular to plate growth is believed to depend on the relative importance of cell boundary and matrix diffusion fluxes. Thus, a high cell boundary migration rate requires a steep concentration gradient across the magnetite/hematite interface and this is best achieved by cell boundary diffusion(12). With increasing temperature, matrix diffusion becomes increasingly important and the concentration gradient normal to the interface should become flatter. Under these conditions, the lengthwise growth of a coherent interface may exceed that of a cellular interface in which case, a plate morphology develops. Presumably, the plates nucleate with a (0001) hematite habit plane because this has an unusually low interfacial energy. However, because of the low mobility of this interface, it appears that sidewise growth at these intermediate temperatures is greater by the cellular mechanism. This leads to the interesting situation in which lengthwise and sidewise growth occur by different mechanisms to produce a morphology analogous to bainite structures in steels. It is interesting to note from Fig. 11 that the cellular reaction tends to proceed first from only one of the two parallel interfaces of a plate nucleus, indicating the important role played by the crystallography in controlling interface mobility.

Conclusions

1. At temperatures below about 650 °C, the reduction of hematite to magnetite proceeds by the migration of a cellular interface along which oxygen and ferrous ions are partitioned by boundary diffusion.

2. A system of tunnels extends from the reaction interface to the outer surface of the hematite and provides an arterial system for the rapid transport of the gas involved in the reaction.
3. At temperatures above about 800 °C, a solid plate-like magnetite product is formed. The lengthwise and sidewise growth of these plates is thought to be controlled by matrix diffusion and interface mobility, respectively.
4. Blocky grains of magnetite are also formed above 800 °C. These have a different orientation relationship from the plates and do not exhibit their pronounced growth anisotropy.
5. At intermediate temperatures (650 - 800 °C), magnetite forms by both cellular and plate growth mechanisms. The main factor responsible for the transition between the two growth modes is thought to be the relative proportion of cell boundary and matrix diffusion fluxes.

Acknowledgement

The authors gratefully acknowledge the encouragement given by Professor J. S. Ball and the provision of the High Voltage Microscope Facilities by the Science Research Council. The work was sponsored by the U.S. Air Force Office of Scientific Research under Grant EOOAR-69-0060.

References

. A. V. Bradshaw, Trans. IMM, 1970, 79, 281-284.

. J. Szekely and J. W. Evans, Blast Furnace Technology, 35-75, Marcel Dekker, New York (1972).

. E. T. Turkdogan and J. V. Vinters, Met. Trans., 1971, 2, 3175-3188.

. F. Habashi, Principles of Extractive Metallurgy, Vol. 1, General Principles, Gordon and Breach, London 1969.

. P. R. Swann and N. J. Tighe, Jernkont.Ann., 1971, 155, 497-501.

. P. R. Swann, in Electron Microscopy and Structure of Materials, 878-903, U. of Calif. Press, Berkeley, 1972.

. D. Turnbull, Acta. Met., 1955, 3, 55-63.

. J. W. Cahn, Acta. Met., 1959, 7, 18-28.

. A. V. Bradshaw and A. G. Matyas, Met. Trans. B, 1976, 81-87.

0. W. A. Johnson and R. F. Mehl, Trans. AIME, 1939, 135, 416-442.

1. J. W. Cahn, Acta. Met., 1956, 4, 449-459.

2. M. Hillert, Mechanisms and Phase Transformations in Crystalline Solids, Institute of Metals, London, 1969.

NBS-114A (REV. 7-73)

U.S. DEPT. OF COMM. **BIBLIOGRAPHIC DATA SHEET**	1. PUBLICATION OR REPORT NO. NBSIR 76-1161	2. Gov't Accession No.	3. Recipient's Accession No.

4. TITLE AND SUBTITLE

High Voltage Microscopy of the Reduction of Hematite to Magnetite

5. Publication Date
December 1976

6. Performing Organization Code

7. AUTHOR(S)
P. R. Swann, N. J. Tighe

8. Performing Organ. Report No.

9. PERFORMING ORGANIZATION NAME AND ADDRESS

NATIONAL BUREAU OF STANDARDS
DEPARTMENT OF COMMERCE
WASHINGTON, D.C. 20234

10. Project/Task/Work Unit No.
3130151

11. Contract/Grant No.
EOAR 69-0067

12. Sponsoring Organization Name and Complete Address *(Street, City, State, ZIP)*
EOAR
223/231
Marylebone Rd.
London, NW1
England

13. Type of Report & Period Covered
Interim 1971-1973

14. Sponsoring Agency Code

15. SUPPLEMENTARY NOTES

16. ABSTRACT *(A 200-word or less factual summary of most significant information. If document includes a significant bibliography or literature survey, mention it here.)*

The microstructural changes associated with the formation of magnetite in hematite have been studied in specimens which have been partially reduced outside the microscope, thinned until electron transparent, and then examined in the normal way. Three types of structure have been observed in varying proportions which depend on the reduction temperature. At low temperatures, magnetite grows by the propagation of a cellular interface, the gas phase being transported to the cell boundary by a network of tunnels. At intermediate temperatures, magnetite plates are formed, whereas at high temperatures, both plate magnetite and blocky magnetite appear. It is proposed that the factor controlling the morphology which develops is the ratio of the cell boundary diffusivity to volume diffusivity of ferrous ions. It is noted that the decomposition morphologies of hematite and austenite have many similarities. The basic reason for this similarity is that both transformations involve substantial redistribution of elements in the solid state and the microstructures which develop are those that perform this redistribution the most efficiently at the temperatures involved.

17. KEY WORDS *(six to twelve entries; alphabetical order; capitalize only the first letter of the first key word unless a proper name; separated by semicolons)*

High voltage electron microscopy, hematite Fe_2O_3, magnetite, Fe_3O_4, gaseous reduction, iron oxide.

18. AVAILABILITY ☒ Unlimited

☐ For Official Distribution. Do Not Release to NTIS

☐ Order From Sup. of Doc., U.S. Government Printing Office
Washington, D.C. 20402, SD Cat. No. C13

☒ Order From National Technical Information Service (NTIS)
Springfield, Virginia 22151

19. SECURITY CLASS (THIS REPORT) UNCLASSIFIED	21. NO. OF PAGES 26
20. SECURITY CLASS (THIS PAGE) UNCLASSIFIED	22. Price $4.00

USCOMM-DC 29042-P74